Journal of Integrative Agriculture 2020, 19(3): 721–734

Available online at www.sciencedirect.com

ScienceDirect

RESEARCH ARTICLE

Growth simulation and yield prediction for perennial jujube fruit tree by integrating age into the WOFOST model

BAI Tie-cheng[1, 2], WANG Tao[2], ZHANG Nan-nan[2], CHEN You-qi[3], Benoit MERCATORIS[1]

[1] *TERRA Teaching and Research Centre, Gembloux Agro-Bio Tech, Liège University, Gembloux 5030, Belgium*

[2] *Southern Xinjiang Research Center for Information Technology in Agriculture/College of Information Engineering, Tarim University, Alaer 843300, P.R.China*

[3] *Institute of Agricultural Resources and Regional Planning, Chinese Academy of Agricultural Sciences, Beijing 100081, P.R.China*

Abstract

Mathematical models have been widely employed for the simulation of growth dynamics of annual crops, thereby performing yield prediction, but not for fruit tree species such as jujube tree (*Zizyphus jujuba*). The objectives of this study were to investigate the potential use of a modified WOFOST model for predicting jujube yield by introducing tree age as a key parameter. The model was established using data collected from dedicated field experiments performed in 2016–2018. Simulated growth dynamics of dry weights of leaves, stems, fruits, total biomass and leaf area index (LAI) agreed well with measured values, showing root mean square error (RMSE) values of 0.143, 0.333, 0.366, 0.624 t ha^{-1} and 0.19, and R^2 values of 0.947, 0.976, 0.985, 0.986 and 0.95, respectively. Simulated phenological development stages for emergence, anthesis and maturity were 2, 3 and 3 days earlier than the observed values, respectively. In addition, in order to predict the yields of trees with different ages, the weight of new organs (initial buds and roots) in each growing season was introduced as the initial total dry weight (TDWI), which was calculated as averaged, fitted and optimized values of trees with the same age. The results showed the evolution of the simulated LAI and yields profiled in response to the changes in TDWI. The modelling performance was significantly improved when it considered TDWI integrated with tree age, showing good global (R^2≥0.856, RMSE≤0.68 t ha^{-1}) and local accuracies (mean R^2≥0.43, RMSE≤0.70 t ha^{-1}). Furthermore, the optimized TDWI exhibited the highest precision, with globally validated R^2 of 0.891 and RMSE of 0.591 t ha^{-1}, and local mean R^2 of 0.57 and RMSE of 0.66 t ha^{-1}, respectively. The proposed model was not only verified with the confidence to accurately predict yields of jujube, but it can also provide a fundamental strategy for simulating the growth of other fruit trees.

Keywords: fruit tree, growth simulation, yield forecasting, crop model, tree age

1. Introduction

Jujube tree (*Zizyphus jujuba*) is mainly planted in the subtropical and tropical regions of Asia, with a history of more than 3 000 years. In China, jujube is mainly distributed in Shandong, Hebei, Shanxi, Shaanxi, Henan provinces and Xinjiang Uygur Autonomous Region, and represented by approximately 3 250 000 ha in 2017

Received 1 February, 2019 Accepted 27 June, 2019
BAI Tie-cheng, E-mail: baitiecheng1983@163.com; Correspondence CHEN You-qi, E-mail: chenyouqi@caas.cn; Benoit MERCATORIS, E-mail: benoit.mercatoris@uliege.be

© 2020 CAAS. Published by Elsevier Ltd. This is an open access article under the CC BY-NC-ND license (http://creativecommons.org/licenses/by-nc-nd/4.0/).
doi: 10.1016/S2095-3119(19)62753-X

(Chinese jujube report 2017, https://baijiahao.baidu.com/s?id=1607747906890869870). Xinjiang has the largest land area devoted to jujube in China, with 1 660 000 km^2, which significantly contributes to jujube supply in terms of quantity and quality due to abundant sunshine and high temperature variations. In addition, jujube fruit is popular due to its high nutritional values, such as vitamin C, amino acids, carbohydrates, and minerals (Li *et al*. 2007), which can be applied to food, food additives and flavourings. It also possesses significant medical values, and is used as a raw material in traditional Chinese medicines with analeptic, palliative and antibechic uses for thousands of years (Li *et al*. 2007). It is also considered as a medicinal supplement, used in tonic medicine and health supplements for blood nourishment and sedation (Gao *et al*. 2013). However, with the increase of planting area, regional growth monitoring and yield prediction has become essential to inform and develop national planting policies and food security strategies.

Most prediction methods for fruit yield still depend on conventional techniques based, for instance, on agro-meteorological models and empirical statistical regressions between spectral vegetation indices and in-field measured yields (Ye *et al*. 2006; Zaman *et al*. 2006; Aggelopoulou *et al*. 2011; Zhou *et al*. 2012; Sun *et al*. 2017; Rahman *et al*. 2018; Bai *et al*. 2019c). One of the main drawbacks of such empirical approaches is that they are only validated for specific cultivars, growth stages, or certain geographical regions (Huang *et al*. 2015b). In contrast, cropping system modelling based on mathematical descriptions of key physical and physiological processes has been considered as a mature technology (Holzworth *et al*. 2014b), and has been applied in precision farming to allow understanding of crop responses in field trials (Asseng *et al*. 2013; Ewert *et al*. 2015; de Wit *et al*. 2019). Such modelling allows better consideration of the complex interactions among plant, weather, soil and agricultural practices (de Wit *et al*. 2019).

In recent decades, many crop models have been developed and constantly optimized for different species and purposes. Some notable examples include WOFOST (WOrld FOod STudies) (van Diepen *et al*. 1989), DSSAT (Decision Support System for Agrotechnology Transfer) (Jones *et al*. 2003), EPIC (Environmental Policy Integrated Climate) (Wang *et al*. 2012), STICS (Multidisciplinary simulator for standard crops) (Brisson *et al*. 2003) and APSIM (Agricultural Production Systems sIMulator) (Holzworth *et al*. 2014a). Among them, the WOFOST model was developed for the quantitative analysis of growth and production of annual field crops, and it has already been in use for 25 years. It has been applied to the study of climate change effects (Alexandrov and Eitzinger 2005; Reidsma *et al*. 2009; Kroes and Supit 2011; Supit *et al*. 2012; Van Walsum and Supit 2012; Reidsma *et al*. 2015; Blanco *et al*. 2017; Gilardelli *et al*. 2018), regional yield forecasting and analysis (Rötter and Van Keulen 1997; Supit *et al*. 1997; Dobermann *et al*. 2000; de Wit *et al*. 2010; Wolf *et al*. 2011; Huang *et al*. 2015a, b, 2016, 2019; Cheng *et al*. 2016; Ceglar *et al*. 2019; Zhou *et al*. 2019), and the comparison of different irrigation and soil conditions (Eitzinger *et al*. 2004; Confalonieri *et al*. 2009; Todorovic *et al*. 2009). It can explain plant growth by using light interception and CO_2 assimilation as the growth driving processes, and includes photosynthesis, respiration and their changes due to environmental conditions (de Wit *et al*. 2005). WOFOST has also been optimized and validated by countless researchers all over the world and used for many new crops over a broad range of climatic and management conditions (de Wit *et al*. 2019). The WOFOST model can be implemented in two different ways: potential production, where crop growth is determined by irradiation, temperature and plant characteristics only; and water-limited production, where crop growth is limited by the water use. Such a crop model can be enriched by remote sensing assimilation data in order to solve scale problems and reduce uncertainties for regional yield forecasting (de Wit *et al*. 2007, 2008, 2012; Curnel *et al*. 2011; Ma *et al*. 2013; Tripathy *et al*. 2013; Liu *et al*. 2015; Huang *et al*. 2019; Zhou *et al*. 2019).

Crop modelling reported in the literature has mainly been developed for annual crops, including spring barley, cotton, maize, millet, potato, rice, sorghum, soybean, sugar beet, sweet potato and winter wheat. However, few studies have focused on perennial fruit trees. An existing study has confirmed that the WOFOST model can be used to simulate jujube growth in field experiments (Bai *et al*. 2019a). However, the yield of such a perennial crop sharply increases with tree age because of the continuous evolution of branches, canopy width, tree height, and leaf area index (He *et al*. 2010). This evolution is mainly reflected by the difference of the initial total dry weight (TDWI), which is directly dependent on tree age. In addition, excessive TDWI values will inevitably result in overestimation of the simulation results if the initial branch weight of the jujube tree was simply added up, therefore, the TDWI parameter shall be redefined for accurate jujube fruit growth modelling. The aim of this study was to develop and evaluate an approach for fruit tree growth dynamic simulation and yield prediction, by integrating the tree age parameter into the WOFOST model. To reach this goal, the following specific objectives were defined:

(1) To explore the methods for growth simulation and yield prediction of perennial jujube trees by redefining and optimizing TDWI.

(2) To evaluate whether the calibrated WOFOST model can be employed to simulate the jujube development accurately from the growth dynamics of different organs

and phenological development stages in specific field experiments.

(3) To validate the accuracy of yield prediction for trees with different ages by comparing simulated yields based on fixed, average, fitted and optimized TDWI with observed yields at a regional scale.

2. Materials and methods

2.1. Field experiment and observed areas

Field experiments were conducted in two jujube orchards located in Alaer City, Xinjiang, China (81°13′2′′E, 40°34′45′′N), during the growing seasons of 2016, 2017 and 2018. In this arid warm-temperate region, the environmental conditions include an average annual rainfall ranging from 40 to 98 mm, a frost-free period from 180 to 224 days and an average photoperiod from April to October of 15 hours. The average annual temperature ranges from 10.8 to 12.5°C, with a maximum daily temperature difference of 20°C, and an accumulated temperature (above 10°C) of 4 105°C. The jujube trees were planted in 2009 in a sandy loam soil. The trees sprouted in mid-April and the fruits were mature in early October (Yang *et al*. 2012).

At a regional scale, 198 jujube production orchards located in the surroundings of the experimental field were observed from 2015 to 2017, in order to consider a broad range of tree ages and validate the model in terms of yield. These orchards were located in four areas (Fig. 1) at a maximum distance of 60 km from the experimental zone. To avoid interference from other factors, the operation management and soil properties of these areas were assumed to be similar because of a small distance between them.

2.2. Study data

Field-scale measurements The proposed model for jujube growth dynamics and production was established based on crop, soil and climatic data measured in the specific experimental fields in 2016 and 2017. The data in 2018 were used for validation of the model. Three datasets, including weather, soil and crop, were carefully prepared. An automatic weather station was 500 m away from the field location, and it measured daily maximum and minimum temperatures, solar radiation, wind speed at 2 m high, actual vapor pressure, and precipitation. The soil physical properties were measured, including average volumetric water content at field capacity, saturated soil moisture content, soil moisture content at wilting point, average bulk density, hydraulic conductivity and water retention parameters, as well as the moisture content at different depths. Measured and observed crop parameters mainly included data related to phenology, leaf area, conversion of assimilates into biomass, maintenance respiration, and partitioning parameters. Moreover, weight of living leaves (WLV, t ha^{-1}), weight of living stems (WST, t ha^{-1}), weight of living storage organs (WSO, t ha^{-1}), weight of aboveground total biomass (TAGP, t ha^{-1}) and leaf area index (LAI, m^2 m^{-2}) were each measured ten times during the growing season

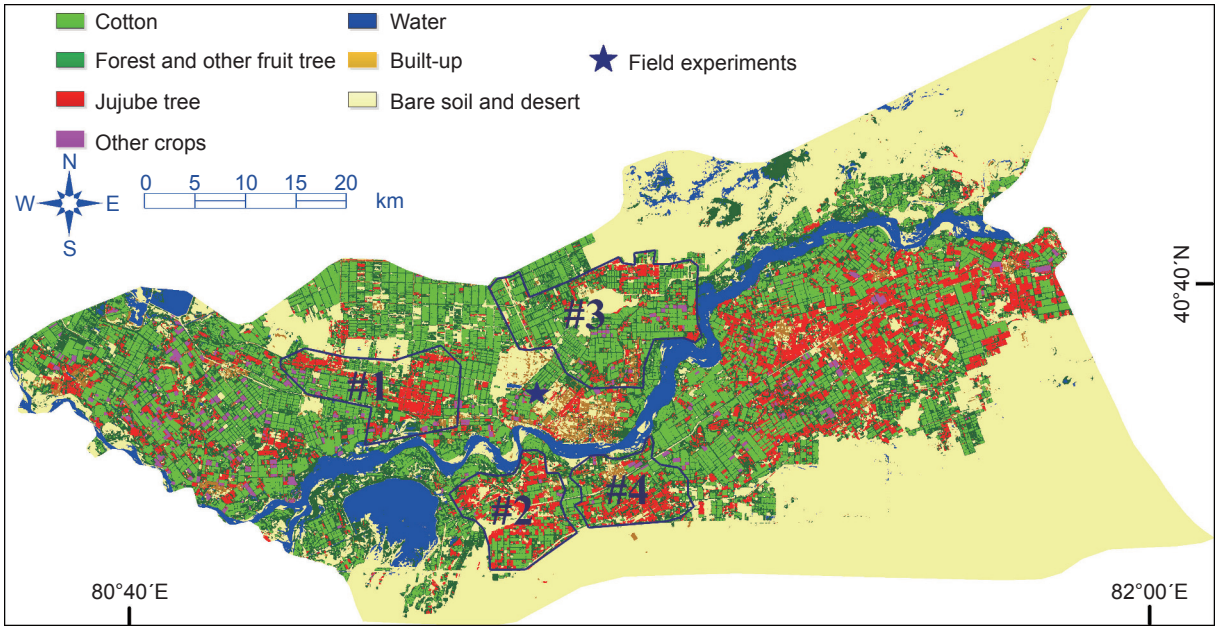

Fig. 1 Location of the experimental zone and observed areas 1 to 4 (processed Landsat 8 image). Source: https://earthexplorer.usgs.gov

for calibration and validation of growth dynamics.

Regional-scale measurements and observations In order to characterize the relationship between TDWI and tree age, the TDWI values of 148 random samples were measured in areas 1 to 4 (Fig. 1) between 2015 and 2017. The datasets were divided into calibration samples (94) and validation samples (54). The statistical values are shown in Table 1.

Yield data from the 198 orchards located in areas 1 to 4 were collected between 2015 and 2017 in order to validate the model at a regional scale (Table 2). Among the data, calibration sets were used to optimize the TDWI of trees with different ages, and validation sets were employed to evaluate modelling capability for yield predictions.

2.3. Model calibration and evaluation method

Before a crop model can be employed for an agro-climatic zone, its parameters must be calibrated and its performance must be validated to ensure that the model can accurately simulate the entire crop growth process by accounting for the variability of various local climatic parameters, soil parameters and crop characteristics (Huang *et al*. 2015b). The model parameters were calibrated based on data measured in field experiments in 2016 and 2017, literature data and empirical values provided by experts. Details of the calibration process for jujube were reported previously (Bai *et al*. 2019a, b). The phenological developmental stages of the model, including emergence, flowering and maturity, were first corrected based on the effective accumulated temperature. According to the rules of the WOFOST model, the phenological development time (stages) of jujube trees needs to be clearly defined. Here, the time when the fifth leaf on the bud was unfolded was defined as the time of emergence (development stage, DVS=0). The time of the first fruit formation was defined as the flowering stage (DVS=1), which is also the time when the fruit production begins to increase. The time when the leaves turned yellow and the dry weight of the fruit remained unchanged was determined as physiological maturity (DVS=2). Then, the measured WLV, WST, WSO,TAGP, and LAI were employed to calibrate other model input parameters, in order to minimize deviations between simulated and measured values. Specifically, CO_2 assimilation parameters can be

Table 1 Statistical values of initial total dry weight (TDWI) in four areas for trees with different ages

TDWI	Average TDWI value of trees with different ages (kg ha^{-1})							
	3rd	4th	5th	6th	7th	8th	9th	10th
Calibration								
Amount	6	10	9	15	10	10	15	19
Max.	5.26	6.49	10.04	13.80	15.30	17.39	20.69	22.46
Min.	4.51	5.59	8.27	12.18	13.55	15.59	17.93	20.57
Mean	4.70	6.10	9.24	13.00	14.28	16.35	19.65	21.59
Validation								
Amount	5	7	7	7	7	5	8	8
Max.	5.42	6.75	10.16	13.85	15.38	17.33	20.65	22.50
Min.	4.63	5.91	8.22	12.61	13.65	15.53	18.99	20.60
Mean	5.09	6.44	9.25	13.49	14.27	16.23	19.88	21.65

Table 2 Yield data from 198 jujube orchards in four areas

Dataset	Site	Cropping season	Average yield of trees with different ages (t ha^{-1})							
			3rd	4th	5th	6th	7th	8th	9th	10th
Calibration										
1	Area 2	2015	5.15	5.97	6.25	8.52	8.08	8.62	9.18	9.47
2	Area 3	2015	4.15	5.19	7.35	7.42	8.21	8.17	8.81	9.18
3	Area 2	2016	4.35	5.10	5.44	6.42	6.62	6.59	7.07	7.15
4	Area 3	2016	3.31	4.49	5.87	6.89	6.83	6.98	7.21	8.17
5	Area 2	2017	4.89	6.77	7.81	8.53	8.25	9.17	9.59	9.97
6	Area 3	2017	5.27	6.15	8.19	8.25	8.67	8.87	9.48	10.62
Validation										
7	Area 1	2015	3.69	5.70	7.88	6.87	8.03	9.02	8.86	7.21
8	Area 4	2015	3.85	5.78	7.81	8.13	8.35	8.45	9.05	9.05
9	Area 1	2016	2.65	4.78	5.39	6.05	7.24	7.02	7.66	8.45
10	Area 4	2016	4.11	5.19	6.85	6.59	6.85	7.51	8.23	7.95
11	Area 1	2017	4.90	4.91	8.24	8.74	8.59	8.29	9.92	9.88
12	Area 4	2017	5.28	6.12	7.49	9.15	8.61	9.05	9.79	10.20

obtained by a fitted light response curve.

The daily gross CO_2-assimilation rate of a crop is calculated from the absorbed radiation and the photosynthesis-light response curve of individual leaves. Net photosynthetic rate can be measured by LI-COR 6400XT (LI-COR, Nebraska, USA). The light response curve at 35.5°C that was fitted by a rectangular hyperbolic correction model (Ye and Yu *et al*. 2007) can be constructed for jujube leaves (Fig. 2, eqs. (1) and (2)). It was confirmed that the fitted results of the rectangular hyperbolic correction model with the minimum root mean square error (RMSE; 0.63 kg ha^{-1} h^{-1}) and almost ideal R^2 (0.998) were superior to those from either rectangular hyperbola (Baly 1935, RMSE=0.997 kg ha^{-1} h^{-1}), non-rectangular hyperbola (Thornley *et al*. 1976, RMSE=0.828 kg ha^{-1} h^{-1}) or exponential equations (RMSE=1.102 kg ha^{-1} h^{-1}). The main CO_2 assimilation parameters characterizing this curve included the initial light use efficiency, α=0.495, the respiration rate in the dark, R_d=2.42, and the maximum rate of net CO_2 assimilation at high light intensity, A_{max}=34.85. Values of α, A_{max}, and R_d at 19.5°C could also be attained in the same way. As assimilation and respiration proceed concurrently, the measured value represents the net assimilation rate, which is the difference between assimilation and respiration. Thus, to obtain the maximum CO_2 assimilation rate (AMAXTB), the measured value should be augmented by the value of the dark respiration implicitly, which assumes that it had the same rate compared to the light respiration (van Diepen *et al*. 1989). Finally, CO_2 assimilation parameters were calculated. The main jujube parameter correction values for potential growth simulations can be found in previous studies (Bai *et al*. 2019b).

$$P_n=\alpha\frac{1-\beta PAR}{1+\gamma PAR}PAR-R_d \quad (1)$$

$$A_{max}=\alpha\left(\frac{\sqrt{\beta+\gamma}-\sqrt{\beta}}{\gamma}\right)^2-R_d \quad (2)$$

where (P_n) is net CO_2 assimilation rate, α is the efficiency of initial light use, β and γ are the fitting coefficients, PAR is the photosynthetic active radiation, and R_d is the respiration rate in the dark. In this study, α=0.495, β=0.000548, γ=0.007887, and R_d=2.423.

The accuracy and agreement between measured and simulated results were quantified using root mean square error (RMSE) and coefficient of determination (R^2), respectively. Their values were calculated by eqs. (3) and (4).

$$\text{RMSE}=\sqrt{\frac{\sum_{i=1}^{n}(\tilde{y}_i-y_i)^2}{n-1}} \quad (3)$$

$$R^2=1-\frac{\sum_{i=1}^{n}(y_i-\tilde{y}_i)^2}{\sum_{i=1}^{n}(y_i-\bar{y}_i)^2} \quad (4)$$

where $\tilde{y}_i$ is the simulated value, y_i is the measured values, $\bar{y}_i$ is the mean of the measured values, and n is the number of samples.

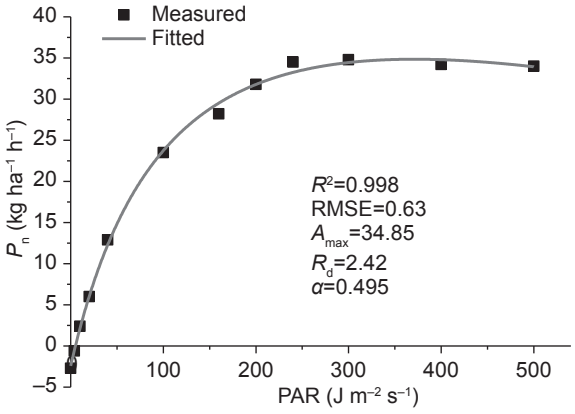

Fig. 2 Light response curve of jujube leaf at 35.5°C. P_n is net CO_2 assimilation rate; PAR is the photosynthetic active radiation.

2.4. Redefinition and calculation of initial total dry weight (TDWI)

Perennial fruit crops are significantly different from annual crops. Jujube trees produce new branches every year and develop fruits on the new branches. With the increase of tree age, the diameter of the trunk increases accordingly, allowing more new branches to be carried. Therefore, the initial TDWI showed strong uncertainty compared to the other input parameters. Therefore, TDWI was redefined as the weight of the initial new organs (initial buds and roots) during each growing season. The initial weight of buds can be calculated by multiplying the average weight of buds retained on each tree and planting density. After that, TDWI can be calculated by the initial weight of buds and partition rate of roots and buds at DVS=0. To reasonably simulate jujube production for trees with different ages, the statistical regression equation between TDWI and tree age was established based on 94 field-measured data samples for calibration and an additional 54 samples for validation. In addition to the fitted TDWI, we also established average and optimized TDWI in consideration of tree age. In this study, TDWI was set as a fixed value regardless of tree age. Where the fixed value was equal to the average of all 148 TDWI samples, the average of the specific age can be calculated using data in Table 1 (for example, the average TDWI of the three-year jujube was equal to 4.8), and the fitted values can be obtained by using the fitted equation between measured TDWI and tree ages. In other words, TDWI could still be optimized by using actual yields for more accurate simulations. A global search algorithm, Girvan–Newman algorithm (GN) (Bickel and Chen 2009),

was employed to optimize the TDWIs. The objective function calculator for the GN algorithm runs the WOFOST model with the given set of input parameters, collects the simulation results and computes the differences with the observations. Different objective functions can be selected, and in this case RMSE´ between measured and simulated yields was carried out for TDWI optimization. The objective function (RMSE´) is shown in eq. (5). A Python optimization code can be accessed at https://nlopt.readthedocs.io/en/latest/:

$$\text{RMSE}' = \sqrt{\frac{\sum_{i=1}^{n}(y_o - y_m)^2}{n}} \quad (5)$$

where y_o represents the observed yield, y_m represents the measured yield, and n represents the number of samples.

The optimized TDWI was determined according to the following rules:

(1) The range was between the minimum and maximum values of the same age (for example, from 4.51 to 5.42 for the 3-year-old tree).

(2) The minimum change interval equaled 0.1 kg ha^{-1}.

(3) The RMSE´ value between the simulated and observed yields was minimal.

3. Results

3.1. Model evaluation in field experiments

Simulation of jujube growth dynamics The indices of agreement between the measured and simulated time series of WLV, WST, WSO and TAGP values are shown in Table 3. Calibrated and validated R^2 for WLV, WST, WSO and TAGP ranged from 0.945 to 0.994 and 0.947 to 0.986, and RMSE from 0.082 to 0.476 t ha^{-1} and 0.143 to 0.624 t ha^{-1}, respectively. Validated results showed the improved model (considering tree age) simulated dynamics for WLV, WST, WSO and TAGP after emergence with better performance than the original model (not considering tree age) (Fig. 3). These parameters were more accurately simulated with an RMSE of 0.143, 0.333, 0.366, and 0.624 t ha^{-1} and an R^2 of 0.947, 0.976, 0.985, and 0.986, respectively. These results preliminarily proved that tree age was a key factor that should be considered when performing a growth simulation of fruit trees.

Fig. 3 also shows the relative deviations of simulated *vs*. measured values, ranging from 0.03 to 0.63 t ha^{-1} for WLV, 0.05 to 0.76 t ha^{-1} for WST, 0.04 to 0.6 t ha^{-1} for WSO and 0.02 to 0.72 t ha^{-1} for TAGP. Note that the first to fourth observations were slightly underestimated for the WLV, WST and TAGP, with high relative deviations. This bias could be attributed to a slightly low ratio of aboveground dry matter to leaves. Therefore, the model generated a low LAI that resulted in a decrease in total photosynthesis accumulation in the early growth period. Considering that the TAGP, WLV, WST and WSO simulations in the later growing season were better, this deviation was acceptable.

LAI was an extremely vital output parameter, which affected photosynthesis and total biomass considerably. Within the calibration datasets, the improved model showed a greater accuracy in simulating LAI values (calibrated R^2=0.98 for 2016, 0.96 for 2017, calibrated RMSE=0.07 for 2016, 0.19 for 2017). Within the validation datasets, the proposed model succeeded in reproducing the timing variability for LAI in the growth period, demonstrated by values of the agreement metrics (validated RMSE=0.19 and R^2=0.95) (Fig. 4). Therefore, this outcome allowed a realistic estimation of light interception and CO_2 assimilation during the main growth duration. In contrast, regardless of tree age, the model indicated a lower ability to generate a time series of simulation, showing an RMSE=0.36 and R^2=0.83. In addition, the simulated LAI change trend was in agreement with the actual growth law of jujube trees. LAI showed an upward trend before fruit white maturity period initially, increasing slowly during emergence duration and then rapidly from late May to early July (during green-up stage), followed by a slight decrease during the maturity period, which peaked at the end of the fruit filling period.

Phenology development validation The simulated time course of total biomass production can be better represented by three phases according to jujube growth characteristics (Table 4). Field validation was employed to describe the errors of simulated emergence, anthesis, and maturity ending date, which were 2, 3 and 3 days

Table 3 Performances of the model in calibration and validation[1)]

Year	Measured TDWI (kg ha^{-1})	R^2 [2)]				RMSE (t ha^{-1})[2)]			
		WLV	WST	WSO	TAGP	WLV	WST	WSO	TAGP
Calibration									
2016	15.1	0.960	0.987	0.993	0.989	0.082	0.173	0.165	0.457
2017	17.2	0.945	0.963	0.994	0.994	0.123	0.360	0.231	0.476
Validation									
2018	19.4	0.947	0.976	0.985	0.986	0.143	0.333	0.366	0.624

[1)] TDWI, initial total dry weight; RMSE, root mean square error.
[2)] WLV, weight of living leaves; WST, weight of living stems; WSO, weight of living storage organs; TAGP, weight of aboveground total biomass.

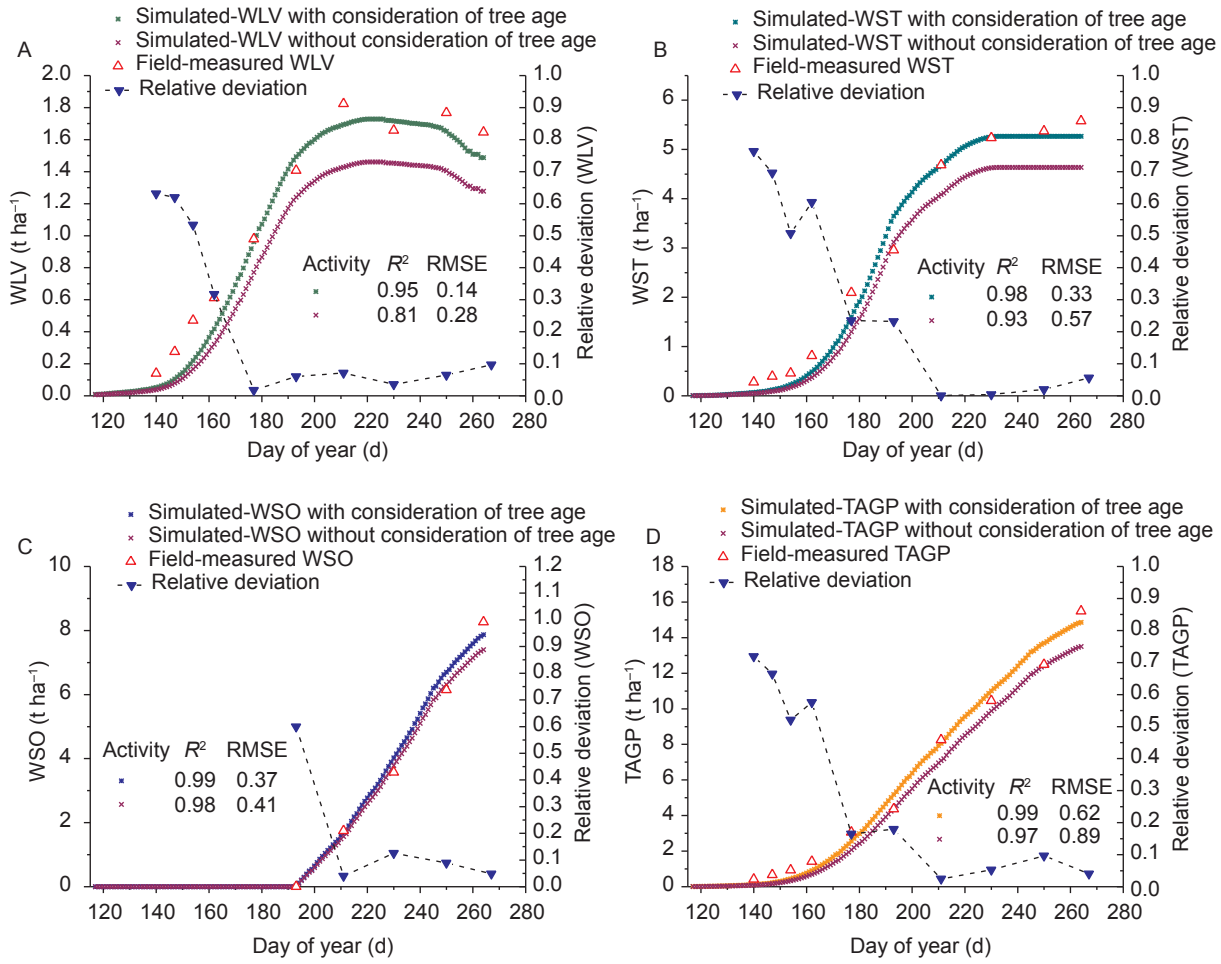

Fig. 3 Simulated *vs*. measured dry weights in 2018 of leaves (A), stems (B), storage organs (C), and aboveground biomass (D) after emergence. Initial total dry weight (TDWI) was equal to a fixed value (average=14.4 t ha^{-1}) regardless of tree age. TDWI was equal to an actual measured value (19.4 t ha^{-1}) when considering tree age. WLV, weight of living leaves; WST, weight of living stems; WSO, weight of living storage organs; TAGP, weight of aboveground total biomass.

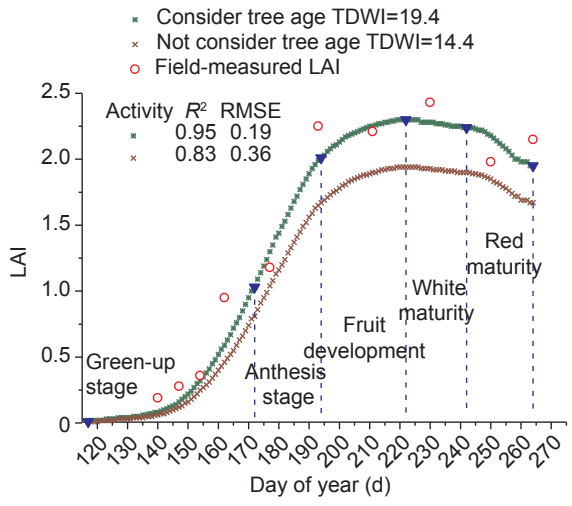

Fig. 4 Simulated and measured leaf area index (LAI) change trends. RMSE, root mean square error.

earlier than the observed values, respectively. In addition, the simulated length of the growth season was one day shorter than the measured value. Therefore, the model had not only accurately reproduced biomass for different organs, but it had gone through a number of phenological development stages, which serve as the controlling and steering mechanism for jujube growth.

Responses to temperature and radiation Depending on the phenological development stage, the model allocated the produced biomass to the different organs. Temperature and radiation changes mainly affected the potential dry weight of different organs. Among them, temperature mainly affected the length of the growing season, including crucial growth duration between DVS=0 and 1 and between DVS=1 and 2 (Table 5), and radiation mainly affected total photosynthesis accumulation.

It should be noted that the temperatures in 2017 were

slightly lower than those in 2016 and 2018, especially in the fruit filling period, so the longer growth period of 9–12 days resulted in higher potential WSO and TAGP (Table 5). Although the time difference between the growth periods in 2016 and 2018 was only two days, the amount of radiation in 2018 (19 516 kJ m^{-2} d^{-1}) was significantly higher than in 2016 (18 875 kJ m^{-2} d^{-1}), which also resulted in a greater TAGP value and yield. Therefore, given that total biomass was determined by growth duration and daily assimilation, the simulated yield in 2017 should be the highest, followed by 2018, and lastly 2016. Both observed and simulated results based on validation datasets agreed with our analysis, demonstrating that the improved model had good temperature and radiation change responses.

3.2. Redefined and calculated TDWI results

The fitted TDWI showed high calibrated and validated correlations (R^2>0.97), and high accuracies (calibrated RMSE=0.813 kg ha^{-1}, validated RMSE=0.893 kg ha^{-1}). Moreover, 39 samples of the validation datasets were standardized in the range between –1 and 1. Note that the fitted equation overestimated TDWI for 4-year-old trees, but underestimated TDWI for 6-year-old trees. Fig. 5 also shows that when the tree age was below 10, TDWI increased with increasing tree age, and TDWI reached the maximum and remained unchanged for trees between 10 and 15 years old. In practice, if the age was greater than 15 years old, TDWI should also be reduced accordingly because the aged branches should usually be replaced by new fruit branches.

Including the fitted TDWI, the values of four kinds of calculated TDWI are shown in Table 6, and the detailed calibrated and validated results are shown in Table 7. Within the calibration datasets, the simulated precision for yield predictions based on optimized TDWI were slightly higher than the average and fitted TDWI (R^2=0.77, RMSE=0.45 t ha^{-1}).

3.3. Effect of TDWI change on LAI and yields

Previous research have indicated that variability of the TDWI parameters strongly influenced the increasing rate of

Table 4 Validation of jujube development stages in 2018

Activity	Emergence stage (d)	Anthesis stage (d)	Red maturity stage (d)
Simulation result	118th	193th	264th
Validation result	120th	196th	267th
Difference	–2	–3	–3

Table 5 Simulated results for the 9-year-old tree[1)]

Year	Average radiation (kJ m^{-2} d^{-1}) in DVS 0–2	Average temperature (°C) in DVS 0–1	Days in DVS 0–1	Average temperature (°C) in DVS 1–2	Days in DVS 1–2	Simulated TAGP (t ha^{-1})	Simulated yield (t ha^{-1})
2016	18 875	23.8	71	23.2	73	13.61	7.338
2017	19 683	23.9	71	21.2	85	16.48	9.320
2018	19 516	22.9	75	23.5	71	15.14	7.950

[1)] DVS 0, 1, 2, development stage at emergence, flowering and maturity, respectively. TAGP, weight of aboveground total biomass.

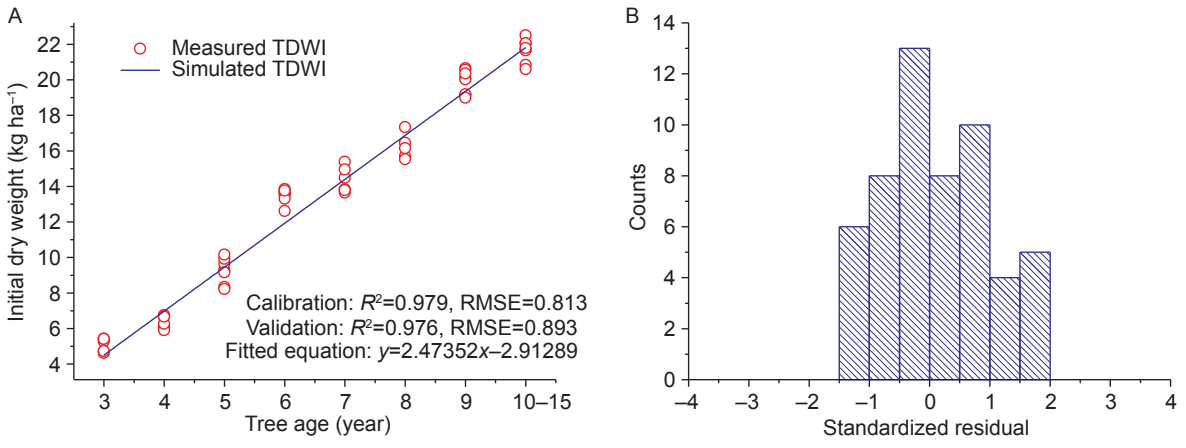

Fig. 5 Fitted equation between initial total dry weight (TDWI) and tree ages (A) and standardized residuals of fitted TDWI (B).

the crop green LAI and max LAI, and further affected crop yield (de Wit *et al*. 2012). In this study, the evolution of the simulated LAI and yields profiled in response to changes in TDWI within the defined ranges are shown in Fig. 6-A and B, respectively. Simulated LAI and yields increased with increasing TDWI, but the ratio of the increase was gradually decreasing, consistent with a previous research result (He *et al*. 2010). In addition, the simulated max LAI for 10-year-old trees in 2017 was 2.44, which showed only a very small deviation from the previous research results (max. LAI=2.58) (Yang *et al*. 2012). In practice, LAI and yields increased rapidly from 3- to 6-year-old trees, then

Table 6 Fixed, average, fitted and optimized initial total dry weight (TDWI) values for different tree ages

Tree age (year)	Fixed TDWI (kg ha^{-1})	Average TDWI (kg ha^{-1})	Fitted TDWI (kg ha^{-1})	Optimized TDWI (kg ha^{-1})
3	14.4	4.88	4.50	4.5
4	14.4	6.24	6.97	6.5
5	14.4	9.24	9.44	10.3
6	14.4	13.23	11.91	13.9
7	14.4	14.23	14.38	15.0
8	14.4	16.30	16.85	17.3
9	14.4	19.73	19.32	20.7
10–15	14.4	21.57	21.79	22.5

Table 7 Contrast of the yields for trees with different ages based on different initial total dry weight (TDWI)

Tree age (year)	Calibrated R^2 [1)]				Validated R^2 [1)]				Calibrated RMSE[1)]				Validated RMSE[1)]			
	a	b	c	d	a	b	c	d	a	b	c	d	a	b	c	d
3	0.55	0.55	0.41	–	0.27	0.27	–	–	0.50	0.50	0.57	3.52	0.79	0.79	0.96	4.00
4	0.75	0.70	0.71	–	0.78	0.82	0.68	–	0.42	0.46	0.45	2.31	0.73	0.35	0.46	2.16
5	0.83	0.80	0.78	0.13	0.47	0.20	0.11	0.44	0.46	0.50	0.53	1.05	0.75	0.93	0.98	0.77
6	0.77	0.50	0.73	0.77	0.80	0.71	0.80	0.80	0.43	0.63	0.47	0.43	0.56	0.68	0.57	0.57
7	0.89	0.88	0.88	0.88	0.80	0.72	0.69	0.72	0.27	0.29	0.29	0.29	0.33	0.39	0.41	0.39
8	0.92	0.92	0.91	0.77	0.52	0.49	0.44	0.07	0.29	0.30	0.32	0.50	0.56	0.58	0.61	0.79
9	0.86	0.82	0.83	0.21	0.47	0.26	0.32	–	0.42	0.48	0.46	1.00	0.64	0.75	0.72	1.37
10–15	0.55	0.51	0.50	–	0.41	0.38	0.37	–	0.84	0.88	0.89	1.62	0.90	0.92	0.92	1.75
Mean	0.77	0.71	0.72	0.35	0.57	0.48	0.43	0.25	0.45	0.51	0.50	1.34	0.66	0.67	0.70	1.48

[1)] a, optimized TDWI; b, fitted TDWI; c, average TDWI; d, fixed TDWI.

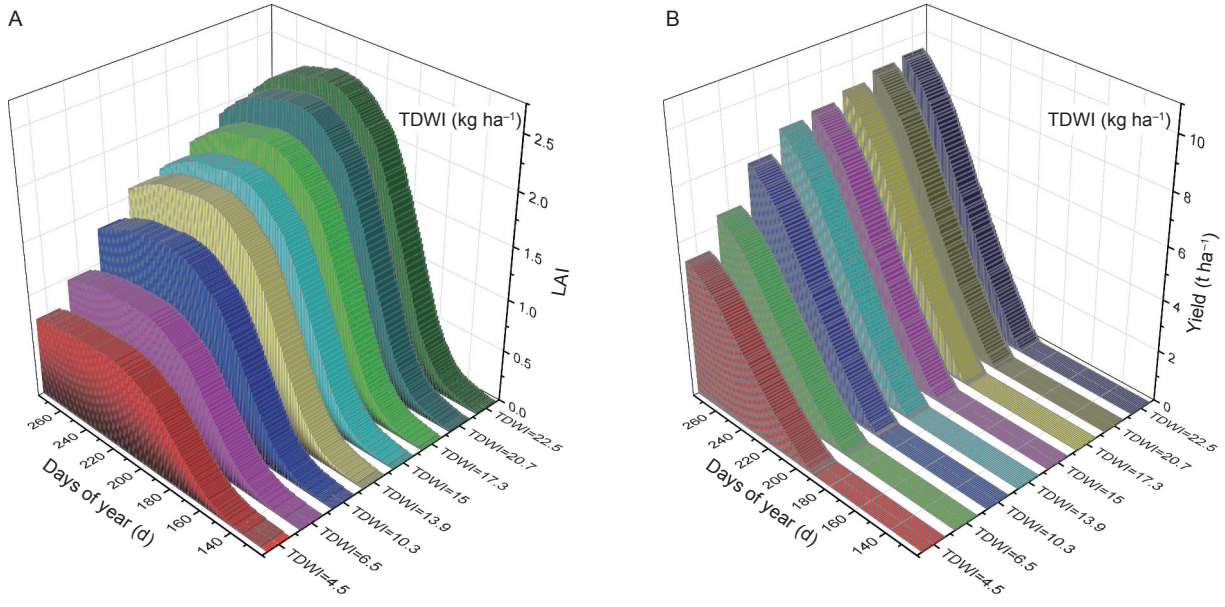

Fig. 6 Change trend of simulated leaf area index (LAI) with tree age in 2017 (A) and Change trend of simulated yields with tree age in 2017 (B). Annual growth rate was equal to yield the difference divided by the initial total dry weight (TDWI) difference.

slowly from 6- to 10-year-old trees, reached the maximum at 10-year-old trees and remained basically unchanged in the subsequent 5 years. The improved model showed a better ability to respond to the influence of TDWI changes on LAI and yields.

3.4. Model evaluation at a regional scale

Global performance validation The comparisons between simulated yields based on four kinds of TDWIs and regional average yields for trees with different ages are presented as scatterplots in Fig. 7. The model showed a greater global accuracy in the calibration datasets than in the evaluation datasets. The modelling accuracy when integrated with any TDWI that considered tree age (average, fitted or optimized TDWI) was significantly higher than that not considering tree age (fixed TDWI), showing higher coefficients of determination (R^2≥0.85) and better accuracy (RMSE≤0.68 t ha^{-1}). Among them, the performance of the optimized TDWI was slightly better than either the average or fitted TDWI, with validated R^2=0.891 and RMSE=0.591 t ha^{-1}.

Local performance validation The modelling capabilities achieved from the four TDWIs for a specific tree age are shown in Table 7. Improved models based on optimized, fitted and average TDWI also showed better performance in predicting jujube yield for a given tree age (average validated R^2=0.57, 0.48, 0.43, RMSE=0.66, 0.67, 0.70 t ha^{-1}, respectively) compared to the fixed TDWI (average R^2=0.25, RMSE=1.48 t ha^{-1}). The model results achieved using the optimized TDWI showed a higher local accuracy rather than either the fitted or the average TDWI, with the exception of the 4-year-old trees. In addition, the model performed slightly worse in the evaluation for 3-year-old (low R^2) and 10–15-year-old trees (higher RMSE). This deviation was attributed to the lower average yield of the 3-year-old trees in 2016 and the 10-year-old trees in 2015 in area 1, which represents an uncertainty.

4. Discussion

The proposed model expresses potential growth simulation, which requires that the crop growth is not limited by water excess or shortage, nutrient shortage, weed competition, or pest and disease infestation (de Wit *et al*. 2019). It is very difficult to achieve in practice. In addition, the methods of collecting regional yield data can still differ in different parts of the region and might not always be accurate (Reidsma *et al*. 2009). Some uncertainties are introduced by the model's architecture. Moreover, the variation of parameters can also lead to considerable uncertainty in yield estimates (Zheng *et al*. 2018). In this study, the method of dynamically adjusting TDWI according to tree ages is employed to effectively reduce the uncertainty of input TDWI.

This study mainly uses a popular planting density. For different planting densities, TDWI values can also be roughly obtained by incorporating the different densities into the formula. Furthermore, two methods can be suggested for improving the accuracy of the model for different planting densities. The first is that the TDWI value can be corrected by regional statistical information for different planting densities. Second, the time series of LAI acquired by remote sensing images with high spatial resolution can be employed to optimize TDWI. After that, the proposed model can be more useful for yield prediction in orchards with different

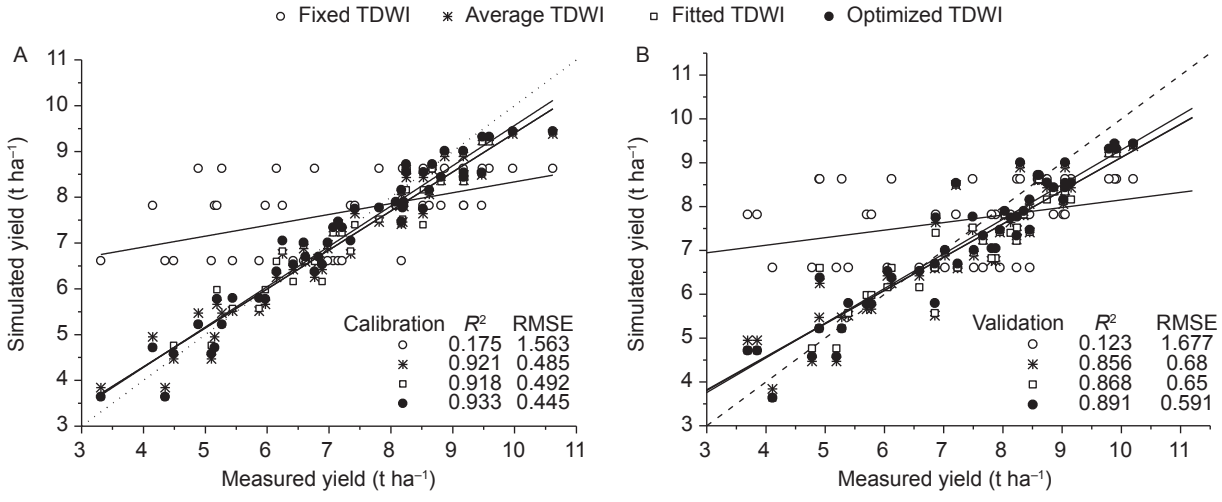

Fig. 7 Global performance of models based on calibration datasets from total 3–15-year-old trees (A) and global validation results based on validation datasets from 3–15-year-old trees (B).

tree ages and planting densities.

The average yield of individual jujube orchards can reach a maximum value of 12 t ha^{-1} for 10-year-old trees. However, the simulated value of the model is only 9.44 t ha^{-1}. This deviation could be interpreted as being influenced by the key input parameters, such as TDWI, and it is calibrated and evaluated using the averages of the different regions in three growth seasons, thus, the simulated results actually represents the average yields of the region and the errors are averaged out. The results also indicate that the errors are more or less normally distributed. In addition, the maximum CO_2 assimilation rate may also increase with the age of the tree (He 2010), so the proposed model underestimates the yield of individual high tree-age orchards and overestimates the yield of low tree-age orchards. In addition, the effect of changes in the atmospheric CO_2 concentration on the simulation results is not initially considered in the WOFOST model. Recent WOFOST implementations correct for the effect by using a CO_2 dependency factor that changes the leaf level maximum assimilation rate (AMAX) and initial light utilization efficiency (EFF) (Vanuytrecht and Thorburn 2017). Moreover, different pruning patterns and quality has a greater impact on the jujube yield, which is a crucial aspect for a reliable fruit simulation. In the process of establishing and correcting model parameters, a small canopy permanent line tree shape widely popularized in Xinjiang was adopted for all orchards. However, there are other tree shapes in actual production management, including cylindrical, a middle trunk shape with three main branches and small canopy permanent trees, and tree shape affects the photosynthetic effect. The yield components of the different tree shapes differs greatly, like mother branches, amount of fruiting branches, single fruit weight and the number of jujubes (Zhang *et al*. 2013). Of course, tree age also contributes to CO_2 flux (He 2010). Accordingly, further analysis and demonstration of the effects of different tree shapes and ages on CO_2 assimilation rate and extinction coefficient would also improve the accuracy of jujube yield estimation. In future work, a time series of reliable LAI acquired by remote sensing images with high spatial resolution could be expected to optimize TDWI, CO_2 assimilation and other sensitive parameters to reduce for the uncertainties of the input parameters.

5. Conclusion

Growth simulation of fruit trees should consider the tree age, which is one of the key factors in accurate simulation. The proposed model is established successfully, based on crop, soil and climatic data measured in field experiments. Results show the model cannot only accurately simulate the biomass of different organs but also reliably present a number of phenological development stages and provide superior climate change response. The research results also demonstrate that the improved models achieved using three kinds of TDWIs (average, fitted, optimized) succeed in forecasting yields of trees with different ages (higher R^2, lower RMSE). Further research on the influences of canopy structure, planting density and tree ages on the CO_2 assimilation is one of most noteworthy aspects, which is expected to improve the prediction accuracy and enhance adaptability. In summary, the method of incorporating tree age into the crop model is not only verified for ensuring the accurate prediction of jujube yields, but can also provide a scheme for modelling growth and yield prediction of other types of fruit trees.

Acknowledgements

This research was supported by the National Natural Science Foundation of China (41561088 and 61501314) and the Science & Technology Nova Program of Xinjiang Production and Construction Corps, China (2018CB020).

References

Aggelopoulou A D, Bochtis D, Fountas S, Swain K C, Gemtos T A, Nanos G D. 2011. Yield prediction in apple orchards based on image processing. *Precision Agriculture*, **12**, 448–456.

Alexandrov V A, Eitzinger J. 2005. The potential effect of climate change and elevated air carbon dioxide on agricultural crop production in central and southeastern Europe. *Journal of Crop Improvement*, **13**, 291–331.

Asseng S, Ewert F, Rosenzweig C, Jones J W, Hatfield J L, Ruane A C, Boote K J, Thorburn P J, Rötter R P, Cammarano D, Brisson N, Basso B, Martre P, Aggarwal P K, Angulo C, Bertuzzi P, Biernath C, Challinor A J, Doltra J, Gayler S, *et al*. 2013. Uncertainty in simulating wheat yields under climate change. *Nature Climate Change*, **3**, 827–832.

Bai T, Zhang N, Chen Y, Mercatoris B. 2019a. Assessing the performance of the WOFOST model in simulating jujube fruit tree growth under different irrigation regimes. *Sustainability*, **11**, 1466.

Bai T, Zhang N, Mercatoris B, Chen Y. 2019b. Improving jujube fruit tree yield estimation at the field scale by assimilating a single landsat remotely-sensed LAI into the WOFOST model. *Remote Sensing*, **11**, 1119.

Bai T, Zhang N, Mercatoris B, Chen Y. 2019c. Jujube yield prediction method combining Landsat 8 Vegetation Index and the phenological length. *Computers and Electronics in Agriculture*, **162**, 1011–1027.

Baly E C C. 1935. The kinetics of photosynthesis. *Proceedings of the Royal Society of London* (Series B: Biological Sciences), **117**, 218–239.

Bickel P J, Chen A. 2009. A nonparametric view of network models and Newman–Girvan and other modularities. *Proceedings of the National Academy of Sciences of the United States of America*, **106**, 21068–21073.

Blanco M, Ramos F, Van Doorslaer B, Martínez P, Fumagalli D, Ceglar A, Fernández F J. 2017. Climate change impacts on EU agriculture: A regionalized perspective taking into account market-driven adjustments. *Agricultural Systems*, **156**, 52–66.

Brisson N, Gary C, Justes E, Roche R, Mary B, Ripoche D, Zimmer D, Sierra J, Bertuzzi P, Burger P, Bussière F, Cabidoche Y M, Cellier P, Debaeke P, Gaudillère J P, Hénault C, Maraux F, Seguin B, Sinoquet H. 2003. An overview of the crop model STICS. *European Journal of Agronomy*, **18**, 309–332.

Ceglar A, van der Wijngaart R, de Wit A, Lecerf R, Boogaard H, Seguini L, van den Berg M, Toreti A, Zampieri M, Fumagalli D, Baruth B. 2019. Improving WOFOST model to simulate winter wheat phenology in Europe: Evaluation and effects on yield. *Agricultural Systems*, **168**, 168–180.

Cheng Z, Meng J, Wang Y. 2016. Improving spring maize yield estimation at field scale by assimilating time-series HJ-1 CCD data into the WOFOST model using a new method with fast algorithms. *Remote Sensing*, **8**, 303.

Confalonieri R, Acutis M, Bellocchi G, Donatelli M. 2009. Multi-metric evaluation of the models WARM, CropSyst, and WOFOST for rice. *Ecological Modelling*, **220**, 1395–1410.

Curnel Y, de Wit A J W, Duveiller G, Defourny P. 2011. Potential performances of remotely sensed LAI assimilation in WOFOST model based on an OSS experiment. *Agricultural and Forest Meteorology*, **151**, 1843–1855.

van Diepen C A, Wolf J, van Keulen H, Rappoldt C. 1989. WOFOST: A simulation model of crop production. *Soil Use Management*, **5**, 16–24.

Dobermann A, Dawe D, Roetter R P, Cassman K G. 2000. Reversal of rice yield decline in a long-term continuous cropping experiment. *Agronomy Journal*, **92**, 633–643.

Eitzinger J, Trnka M, Hösch J, Žalud Z, Dubrovský M. 2004. Comparison of CERES, WOFOST and SWAP models in simulating soil water content during growing season under different soil conditions. *Ecological Modelling*, **171**, 223–246.

Ewert F, Rötter R P, Bindi M, Webber H, Trnka M, Kersebaum K C, Olesen J E, van Ittersum M K, Janssen S, Rivington M, Semenov M A, Wallach D, Porter J R, Stewart D, Verhagen J, Gaiser T, Palosuo T, Tao F, Nendel C, Roggero P P, *et al*. 2015. Crop modelling for integrated assessment of risk to food production from climate change. *Environmental Modelling and Software*, **72**, 287–303.

Gao Q, Wu C, Wang M. 2013. The Jujube (*Ziziphus Jujuba* Mill.) fruit: A review of current knowledge of fruit composition and health benefits. *Journal of Agricultural and Food Chemistry*, **61**, 3351–3363.

Gilardelli C, Confalonieri R, Cappelli G A, Bellocchi G. 2018. Sensitivity of WOFOST-based modelling solutions to crop parameters under climate change. *Ecological Modelling*, **368**, 1–14.

He T. 2010. Study on the configuration and light distribution characteristics in slope-land jujube plantation of north Shaanxi, Yangling. MSc thesis, Northwest A&F University, Yanglin, Shaanxi, China. (in Chinese)

Holzworth D P, Huth N I, deVoil P G, Zurcher E J, Herrmann N I, McLean G, Chenu K, van Oosterom E J, Snow V, Murphy C, Moore A D, Brown H, Whish J P M, Verrall S, Fainges J, Bell L W, Peake A S, Poulton P L, Hochman Z, Thorburn P J, *et al*. 2014a. APSIM — Evolution towards a new generation of agricultural systems simulation. *Environmental Modelling and Software*, **62**, 327–350.

Holzworth D P, Snow V, Janssen S, Athanasiadis I N, Donatelli M, Hoogenboom G, White J W, Thorburn P. 2014b. Agricultural production systems modelling and software: Current status and future prospects. *Environmental Modelling and Software*, **72**, 276–286.

Huang J, Ma H, Sedano F, Lewis P, Liang S, Wu Q, Su W, Zhang X, Zhu D. 2019. Evaluation of regional estimates of winter wheat yield by assimilating three remotely sensed reflectance datasets into the coupled WOFOST–PROSAIL model. *European Journal of Agronomy*, **102**, 1–13.

Huang J, Ma H, Su W, Zhang X, Huang Y, Fan J, Wu W. 2015a. Jointly assimilating MODIS LAI and ET products into the SWAP model for winter wheat yield estimation. *IEEE Journal of Selected Topics in Applied Earth Observations and Remote Sensing*, **8**, 4060–4071.

Huang J, Sedano F, Huang Y, Ma H, Li X, Liang S, Tian L, Zhang X, Fan J, Wu W. 2016. Assimilating a synthetic Kalman filter leaf area index series into the WOFOST model to improve regional winter wheat yield estimation. *Agricultural and Forest Meteorology*, **216**, 188–202.

Huang J, Tian L, Liang S, Ma H, Becker-Reshef I, Huang Y, Su W, Zhang X, Zhu D, Wu W. 2015b. Improving winter wheat yield estimation by assimilation of the leaf area index from Landsat TM and MODIS data into the WOFOST model. *Agricultural and Forest Meteorology*, **204**, 106–121.

Jones J W, Hoogenboom G, Porter C H, Boote K J, Batchelor W D, Hunt L A, Wilkens P W, Singh U, Gijsman A J, Ritchie J T. 2003. The DSSAT cropping system model. *European Journal of Agronomy*, **18**, 235–265.

Kroes J G, Supit I. 2011. Impact analysis of drought, water excess and salinity on grass production in the netherlands using historical and future climate data. *Agriculture, Ecosystems and Environment*, **144**, 370–381.

Li J, Fan L, Ding S, Ding X. 2007. Nutritional composition of five cultivars of Chinese jujube. *Food Chemistry*, **103**, 454–460.

Liu F, Liu X, Ding C, Wu L. 2015. The dynamic simulation of rice growth parameters under cadmium stress with the assimilation of multi-period spectral indices and crop model. *Field Crops Research*, **183**, 225–234.

Ma G, Huang J, Wu W, Fan J, Zou J, Wu S. 2013. Assimilation of MODIS-LAI into the WOFOST model for forecasting regional winter wheat yield. *Mathematical and Computer Modelling*, **58**, 634–643.

Rahman M M, Robson A, Bristow M. 2018. Exploring the potential of high resolution WorldView-3 imagery for estimating yield of mango. *Remote Sensing*, **10**, 1866.

Reidsma P, Ewert F, Boogaard H, van Diepen K. 2009. Regional crop modelling in Europe: The impact of climatic conditions and farm characteristics on maize yields. *Agricultural Systems*, **100**, 51–60.

Reidsma P, Wolf J, Kanellopoulos A, Schaap B F, Mandryk M, Verhagen J, Van Ittersum M K. 2015. Climate change impact and adaptation research requires integrated assessment and farming systems analysis: A case study in the Netherlands. *Environmental Research Letters*, **10**, 045004.

Rötter R, Van Keulen H. 1997. Variations in yield response to fertilizer application in the tropics: II. Risks and opportunities for smallholders cultivating maize on Kenya's arable land. *Agricultural Systems*, **53**, 69–95.

Sun L, Gao F, Anderson M C, Kustas W P, Alsina M M, Sanchez L, Sams B, McKee L, Dulaney W, White W A, Alfieri J G, Prueger J H, Melton F, Post K. 2017. Daily mapping of 30 m LAI and NDVI for grape yield prediction in California vineyards. *Remote Sensing*, **9**, 317.

Supit I. 1997. Predicting national wheat yields using a crop simulation and trend models. *Agricultural and Forest Meteorology*, **88**, 199–214.

Supit I, van Diepen C A, de Wit A J W, Kabat P, Baruth B, Ludwig F. 2012. Assessing climate change effects on European crop yields using the crop growth monitoring system and a weather generator. *Agricultural and Forest Meteorology*, **164**, 96–111.

Thornley J H M. 1976. Mathematical models in plant physiology. Academic Press London. [2018-12-10]. https://www.cabdirect.org/cabdirect/abstract/19760343677

Todorovic M, Albrizio R, Zivotic L, Abi Saab M T, Stöckle C, Steduto P. 2009. Assessment of Aquacrop, Cropsyst, and WOFOST models in the simulation of sunflower growth under different water regimes. *Agronomy Journal*, **101**, 509–521.

Tripathy R, Chaudhari K N, Mukherjee J, Ray S S, Patel N K, Panigrahy S, Parihar J S. 2013. Forecasting wheat yield in Punjab State of India by combining crop simulation model WOFOST and remotely sensed inputs. *Remote Sensing Letters*, **4**, 19–28.

Vanuytrecht E, Thorburn P J. 2017. Responses to atmospheric CO_2 concentrations in crop simulation models: A review of current simple and semicomplex representations and options for model development. *Global Change Biology*, **23**, 1806–1820.

Van Walsum P E V, Supit I. 2012. Influence of ecohydrologic feedbacks from simulated crop growth on integrated regional hydrologic simulations under climate scenarios. *Hydrology and Earth System Sciences*, **16**, 1577–1593.

Wang X, Williams J R, Gassman P W, Baffaut C, Izaurralde R C, Jeong J, Kiniry J R. 2012. EPIC and APEX: Model use, calibration, and validation. *Transactions of the ASABE*, **55**, 1447–1462.

de Wit A, Baruth B, Boogaard H, Van Diepen K, Van Kraalingen D, Micale F, Te Roller J, Supit I, Van Den Wijngaart R. 2010. Using ERA-INTERIM for regional crop yield forecasting in Europe. *Climate Research*, **44**, 41–53.

de Wit A, Boogaard H, Fumagalli D, Janssen S, Knapen R, van Kraalingen D, Supit I, van der Wijngaart R, van Diepen K. 2019. 25 years of the WOFOST cropping systems model. *Agricultural Systems*, **168**, 154–167.

de Wit A, Boogaard H L, Diepen C A V. 2005. Spatial resolution of precipitation and radiation: The effect on regional crop yield forecasts. *Agricultural and Forest Meteorology*, **135**, 156–168.

de Wit A, van Diepen C A. 2007. Crop model data assimilation with the ensemble kalman filter for improving regional crop yield forecasts. *Agricultural and Forest Meteorology*, **146**, 38–56.

de Wit A, van Diepen C A. 2008. Crop growth modelling and crop yield forecasting using satellite-derived meteorological inputs. *International Journal of Applied Earth Observation and Geoinformation*, **10**, 414–425.

de Wit A, Duveiller G, Defourny P. 2012. Estimating regional winter wheat yield with WOFOST through the assimilation of green area index retrieved from MODIS observations. *Agricultural and Forest Meteorology*, **164**, 39–52.

Wolf J, Hessel R, Boogaard H L, De Wit A, Akkermans W, van Diepen C A. 2011. Modelling winter wheat production across Europe with WOFOST — The effect of two new zonations and two newly calibrated model parameter sets. In: Ahuja L R, Ma L, eds. *Methods of Introducing System Models into Agricultural Research.* American Society of Agronomy. Crop Science Society of America, Soil Science Society of America. https://doi.org/10.2134/advagricsystmodel2.c11

Yang W, Gao J, Xu C. 2012. The correlation analysis of leaf area index and yield of red jujube. *Xinjiang Agricultural Sciences*, **49**, 1397–1400. (in Chinese)

Ye X, Sakai K, Garciano L O, Asada S I, Sasao A. 2006. Estimation of citrus yield from airborne hyperspectral images using a neural network model. *Ecological Modelling*, **198**, 426–432.

Ye Z, Yu Q. 2007. Comparison of a new model of light response of photosynthesis with traditional models. *Journal of Shenyang Agricultural University*, **38**, 771–775. (in Chinese)

Zaman Q U, Schumann A W, Hostler H K. 2006. Estimation

of citrus fruit yield using ultrasonically-sensed tree size. *Applied Engineering in Agriculture*, **22**, 39–44.

Zhang Q, Bai T, Wu C. 2013. Investigation on yield and quality of jujube in different tree shapes in direct seeding and orchard construction. *Northern Horticulture*, **4**, 18–23. (in Chinese)

Zheng Y, Li Z, Xiao J, Yuan W, Yan M, Li T, Zhang Z. 2018. Sources of uncertainty in gross primary productivity simulated by light use efficiency models: Model structure, parameters, input data, and spatial resolution. *Agricultural and Forest Meteorology*, **263**, 242–257.

Zhou G, Liu X, Liu M. 2019. Assimilating remote sensing phenological information into the WOFOST model for rice growth simulation. *Remote Sensing*, **11**, 268.

Zhou R, Damerow L, Sun Y, Blanke M M. 2012. Using colour features of *cv*. 'Gala' apple fruits in an orchard in image processing to predict yield. *Precision Agriculture*, **13**, 568–580.

Executive Editor-in-Chief HUANG San-wen
Managing editor WENG Ling-yun